Running-in effect on the load-carrying capacity of a water-lubricated SiC thrust bearing

X Wang, K Kato and K Adachi

Proceedings of the Institution of Mechanical Engineers, Part J: Journal of Engineering Tribology 2005 219: 117
DOI: 10.1243/135065005X9727

Running-in effect on the load-carrying capacity of a water-lubricated SiC thrust bearing

X Wang*, **K Kato,** and **K Adachi**
Laboratory of Tribology, School of Mechanical Engineering, Tohoku University, Sendai, 980-8579, Japan

The manuscript was received on 27 November 2002 and was accepted after revision for publication on 5 November 2004.

DOI: 10.1243/135065005X9727

Abstract: It is known the friction of self-mated SiC in water strongly depends on the roughness of their contact surfaces, and a proper running-in process is the way to obtain low friction by smoothing the contact surfaces of SiC with tribochemical wear. In this paper, the running-in process of surface-contacted SiC (thrust-bearing-type contact) in water is studied experimentally. It is found the maximum running-in load has a large influence on the load-carrying capacity, which is measured as the critical load for the transition from hydrodynamic to mixed lubrication in this research. A multi-step loading running-in method is proposed to increase the load-carrying capacity of SiC thrust bearings working in water. Finally, the running-in process of a laser textured SiC surface is studied, the effect of the pore area ratio on the roughness of the run-in surface is reported, and the mechanism of the effect of micropores is discussed.

Keywords: running-in, SiC, load-carrying capacity, water lubrication, surface texture

1 INTRODUCTION

Silicon carbide (SiC) has become a most important material for sliding bearings and mechanical seals working in water due to its excellent physical properties and high load-carrying capability [**1–3**]. In particular, the low friction even under water lubrication makes it possible to realize oil-free lubrication, which saves resources and decreases the pollution in the earth.

It is known that the tribochemical reaction is the key for establishing low friction of silicon-based ceramics sliding in water. The hard surfaces of Si_3N_4 and SiC are able to become very smooth by tribochemical wear [**4**], and the reaction product, silicon oxide, will dissolve in water to generate a soft layer, which increases the real contact area to decrease the contact pressure and acts as a lubricant to reduce friction [**5**].

The surface roughness of SiC has such a large influence on the friction coefficient that it is said that the initial dynamic coefficient of friction reflects the initial roughness of the mating surfaces [**6**, **7**]. In order to obtain a friction coefficient lower than 0.01 for on SiC thrust contact in water, a roughness R_{rms} lower than 0.08 μm is necessary [**8**]. This roughness could be obtained by supersurface finishing and a running-in process.

The transition of the wear mode from mechanically dominated wear to tribochemically dominated wear has been found in the running-in process of both Si_3N_4 and SiC sliding in water [**9**, **10**]. Si_3N_4 seems to make this transition so easily that low friction was observed in almost all the experiments documented by Tomizawa and Fischer [**4**], Sasaki [5], Xu *et al.* [**10**]. However, for SiC sliding in water, the friction coefficient obtained by Tomizawa and Fischer [**4**] is 0.26 (5 N; 0–0.2 m/s; pin on disc), while low friction ($\mu < 0.01$) was observed by Sasaki [**5**] (50 N; 0.1–0.8 m/s, pin on disc) and Wong *et al.* [**8**] (0–600 N, 1000 r/min; ring on disc).

The results obtained by Chen *et al.* [**11**] possibly gave an explanation for these phenomena. The pin-on-disc experiments were carried out with a load of 5 N and a sliding speed of 120 mm/s; the friction coefficient of Si_3N_4 changes from 0.95 to 0.0035 after 16 000 cycles, while SiC needs more than 68 000 cycles for a decrease in the friction coefficient

Corresponding author: National Institute of Standards and Technology, Building 223, 100 Bureau Drive, Gaithersburg, MD, 2089 8520, USA.

from 0.45 to 0.01. During these running-in processes, Si_3N_4 exhibits mainly tribochemical wear but, for SiC there is a clear transition from mechanical wear to tribochemical wear [**12**]. This implies that the number of cycles necessary and the appropriate wear mode need to be controlled to obtain low friction during the running-in process of SiC in water.

However, for surface-contacted SiC, most documented experiments were only carried out at fixed loads selected arbitrarily or based on the results of pin-on-disc tests. The effect of the running-in process on the performance of surface-contacted SiC is still unclear.

Therefore, the purpose of this research is to study the running-in load effect on the load-carrying capacity of SiC in a thrust-bearing-type contact sliding in water.

Surface texturing has proved to be an effective way to increase the load-carrying capacity of the SiC surface. As well as the additional hydrodynamic pressure generated by surface texture, the water storage ability of surface texture is assumed to be helpful for the tribochemical reaction on the contact surfaces of SiC [**13**, **14**]. The effect of surface texture on the running-in process is also studied experimentally. The mechanism of increasing the load-carrying capacity of the SiC thrust bearing by surface texture is discussed from the viewpoint of the running-in process.

2 EXPERIMENTAL PROCEDURE

2.1 Specimens

The sliding tests were performed between the flat surfaces of a ring (Fig. 1a) and a disc (Fig. 1b). Both the disc and the ring were made of SiC, which was sintered without pressurization. The physical properties of the SiC used are shown in Table 1. The centre hole of the ring was used for water supply. Two grooves were made on the flat surface of the ring to guide water from the centre hole to the contact surfaces. This type of contact is similar to that of thrust bearings. The contact area of the ring and disc is about 1.9 cm^2.

Table 1 Physical properties of SiC sintered without pressurization

Density	3100 kg/m^3
Bending strength	470 MPa
Vickers hardness	2800
Coefficient of thermal expansion	4.02×10^{-6} K
Thermal conductivity	125.6 W/m K

Both the flat surfaces of the ring and the disc were ground to a roughness R_{rms} of around 0.2 μm before testing. Figure 2 shows an example of the surface profile after grinding. Figure 3 shows a typical surface topography measured by atomic force microscopy.

Laser-textured discs were also used to investigate the effect of micropores on the running-in process. The pores were arranged in square array shown in Fig. 4 by a CO_2 laser. The diameter and depth of the pores were determined according to the power and pulse width of the laser. The interval between the pores was changed to obtain a series of pore area ratios. In this research, the pore area ratio was in the range from 2.8 to 22.5 per cent. After laser treatment, the flat surface of the disc was ground again to remove the bulges formed on the rims of the pores.

Figure 5 shows a scanning electron micrograph and cross-sectional profile of a pore after final grinding.

2.2 Apparatus

Figure 6 shows the apparatus used in this experiment.

The ring is mated to the disc and driven by a motor to a certain rotational speed which could be adjusted in the range 200–1500 r/min. The disc is supported by a half-spherical tip so that its flat surface is

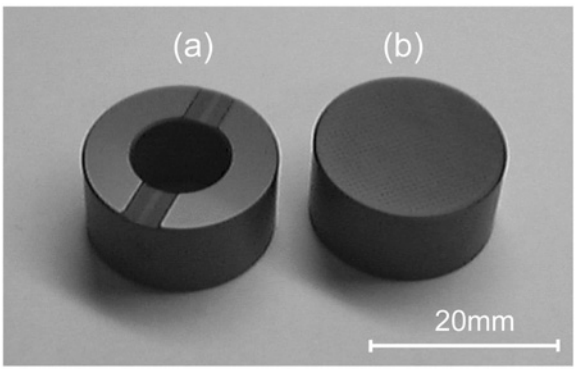

Fig. 1 The SiC specimens: (a) ring; (b) disc

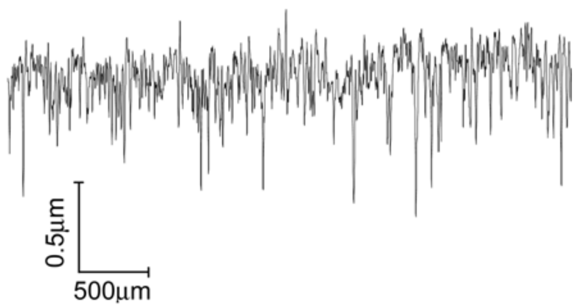

Fig. 2 A typical surface profile of the ring and disc after grinding

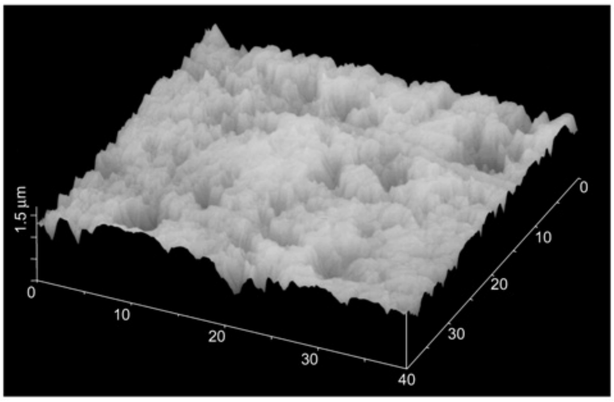

Fig. 3 Typical surface topography of the ring and disc after grinding

automatically aligned to match the flat surface of the ring. The load is applied by a hydraulic system from the bottom of the disc. Purified water is supplied to the centre hole of the ring with a flow rate of 60 ml/min. The temperature of the water supplied to the friction surfaces was controlled at around 18 °C. The load and frictional torque are detected by load cells. An air bearing is used to support the disc so that very small frictional torque (less than 0.001 N m) can be detected accurately.

An autostop system is used to stop the load-applying system and the driving motor to avoid damage to apparatus and specimens when the frictional torque increases rapidly.

3 EXPERIMENTAL RESULTS

3.1 Multi-step loading running-in process

As mentioned above, an appropriate load and sliding speed, at which tribochemical wear is induced as the dominant wear mode, are capable of generating smooth surfaces during the running-in period of SiC in water. Figure 7a shows the response of the frictional force to the load increase at the initial stage of running-in at 1000 r/min. After the load of about 100 N is increased, the frictional force rapidly rises to a high value, then falls with the passage of sliding time and finally tends to a stable value. This is an efficient running-in process since it only takes about 5 min for the frictional force to decrease by half because of the improvement to the contact

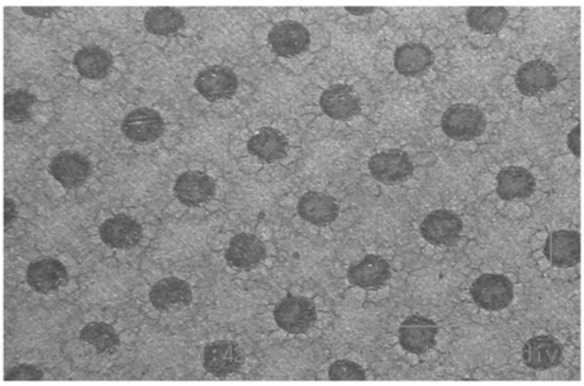

Fig. 4 The arrangement of micropores on the surface of a disc

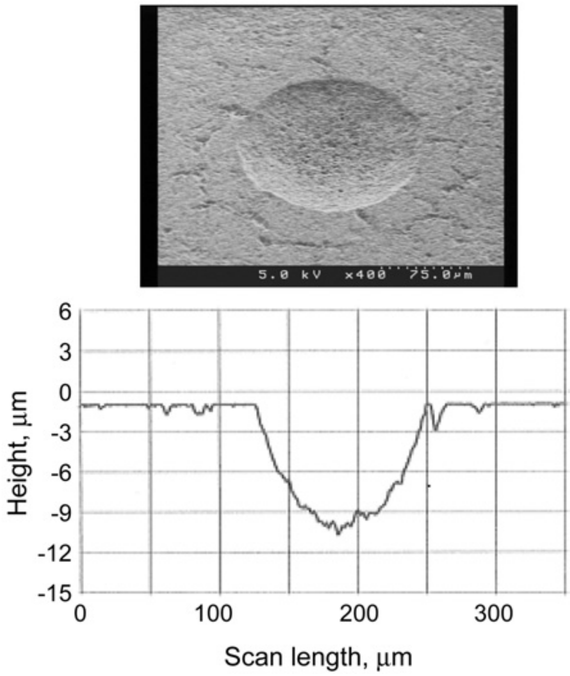

Fig. 5 Scanning electron micrograph and cross section profile of a micropore produced by laser

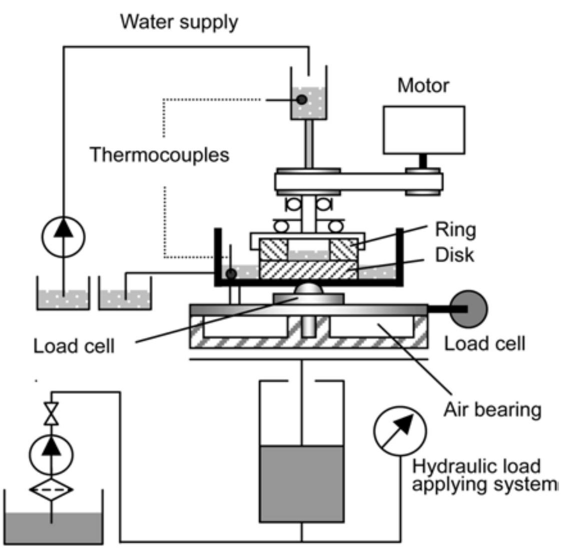

Fig. 6 Schematic diagram of the apparatus for the ring-on-disc test

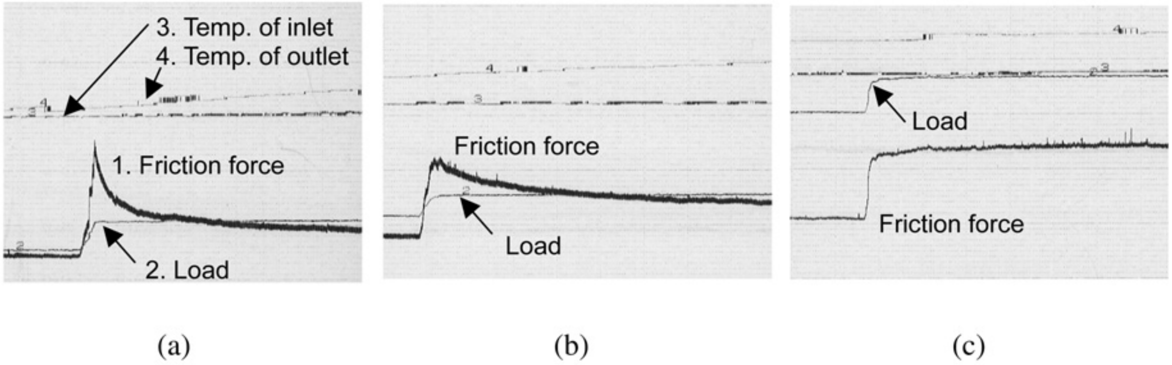

Fig. 7 The friction properties of the SiC ring on disc during the running-in process in water with a rotational speed of 1000 r/min

conditions due to wear. At the moment when the load is increased, an increase in the load from 100 N to 200 N brings about an increase in the frictional force to a value four times that of the previous value. This rapidly increasing rate of the frictional force indicates that, in order to avoid brittle fracture on the surface as a result of the high friction, the high load in the running-in process should be applied in a step-by-step manner instead of all at once.

After several steps of load increase, the decreasing rate of the frictional force become increasingly slower, as shown in Fig. 7b. More sliding time is required to obtain a near-stable frictional force than in the initial running-in stage.

Finally, no obvious decrease can be found after a higher load is applied to the contact. Figure 7c shows a typical curve of frictional force in this case. However, sometimes the frictional force becomes unstable, or it still keeps decreasing at a very slow rate. The former also implies that contact conditions could no longer be improved in these conditions so that it is meaningless to continue the running-in process. In the latter case, the load could be applied continuously until the appartus limits are reached.

Figure 8 shows a typical surface topography after such a running-in process. No deformation and no brittle fracture of the materials occurs on the surface. The peaks before running-in have been 'cut' so neatly by tribochemical wear that the bearing area is increased significantly.

3.2 Running-in process versus load-carrying capacity

Figure 9 shows the friction properties of a SiC ring on disc in water after the multi-step loading running-in process with maximum loads of 300 N and 1200 N respectively. The friction coefficient in both cases stays low ($\mu < 0.01$) while the load is light and then begin to increase rapidly from the loads W_c of about 250 N and 1100 N respectively. Since the friction coefficient in the low-friction range is below 0.01, it is reasonable to consider the load W_c as the critical load at which the transition from hydrodynamic to mixed lubrication happens. A higher critical load means that this 'thrust bearing' has a higher load-carrying capacity since it can work with low friction within a wider load range. Therefore, the critical load W_c is used for evaluation of the load-carrying capacity in this research.

It is found that different running-in loads result in different load-carrying capacities of this thrust contact.

Figure 10 shows the effect of the maximum running-in load on the critical load W_c. The near-linear relationship indicates that, in order to have a high load-carrying capacity, it is necessary to carry out the running-in process on the contact surface with a load that is as high as possible.

3.3 Running-in process of the textured SiC surface

A series of laser-textured specimens with different pore area ratios were tested to find the optimum texture pattern for the high load-carrying capacity.

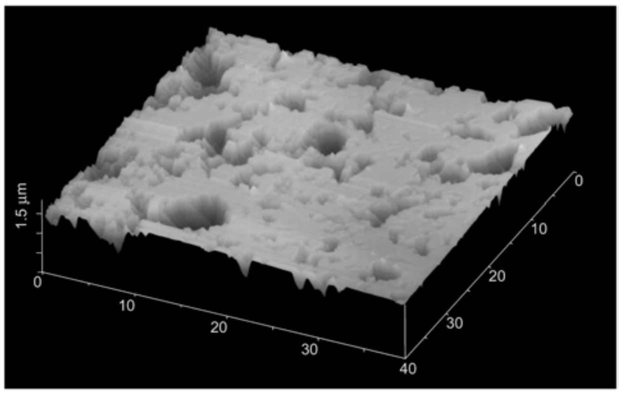

Fig. 8 Typical surface topography of a SiC ring and disc after running in

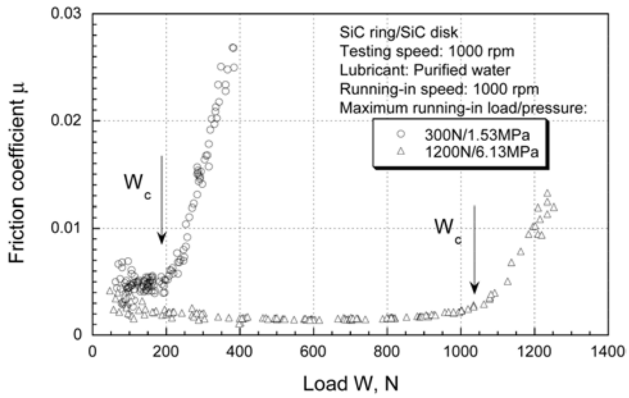

Fig. 9 The friction properties of the SiC ring on disc in water after running in with maximum loads of 300 N and 1200 N

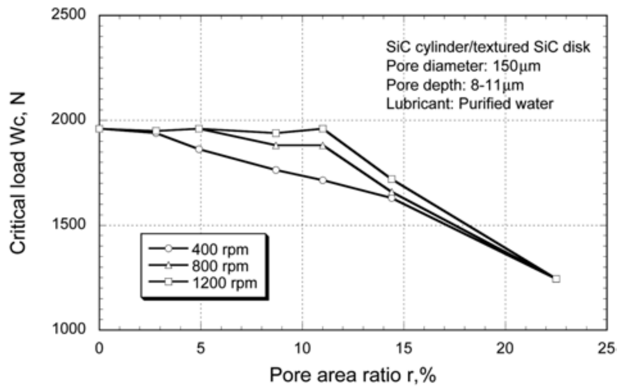

Fig. 11 The critical load after running in with a maximum load of 2000 N (pressure, 10.2 MPa) ($r < 12$ per cent) or less ($r > 12$ per cent)

It was planned to carry out the same multi-step running-in process for all the specimens before testing. The rotational speed was 1000 r/min. The maximum load was set to 2000 N. For the specimens with pore area ratios below 12 per cent, the running-in processes were performed up to a load of 2000 N. However, for specimens with pore area ratios of 14.4 per cent and 22.5 per cent, the running-in processes had to be stopped at loads of about 1800 N and 1300 N respectively since running-in was not able to advance any more in those cases.

Figure 11 shows the critical load W_c at 400 r/min, 800 r/min, and 1200 r/min after such a running-in process. For the specimens with the pore area ratios of 14.4 per cent and 22.5 per cent, the critical loads are quite different. However, for the specimens with pore area ratios below 12 per cent, there is almost no difference in the critical load at 1200 r/min. This indicates that the same running-in process will result in almost the same load-carrying capacity. The difference in the critical load, of these specimens at a rotational speed of 400 r/min is possibly because the testing speed is far from the running-in speed.

Therefore, these specimens were run in again to a load that is as high as possible. Then, their critical load were measured again. The results are shown in Fig. 12.

It is found that the different pore area ratios result in different amounts of progress of the running-in process, which leads to different critical loads. The specimen with a pore area ratio of around 3 per cent has the highest running-in load, which causes the highest critical load of about 2500 N at a rotational speed of 1200 r/min. This is about 20 per cent higher than that of the untextured specimen.

Figure 13 shows the roughness of the surface around micropores after the running-in process described above. The average value of every specimen was calculated from eight measurements on

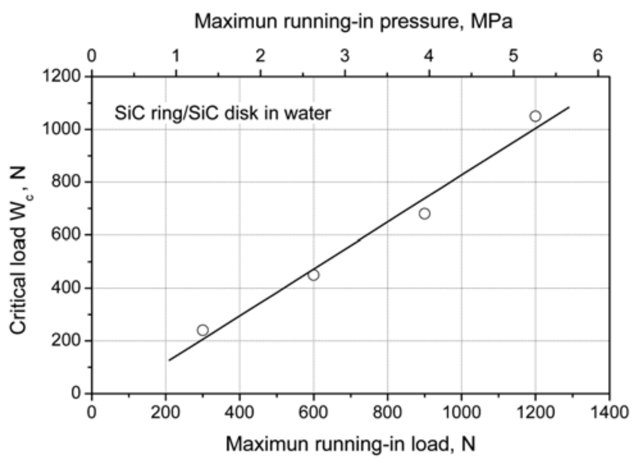

Fig. 10 The effect of maximum running-in load on the critical load for the transition from hydrodynamic to mixed lubrication

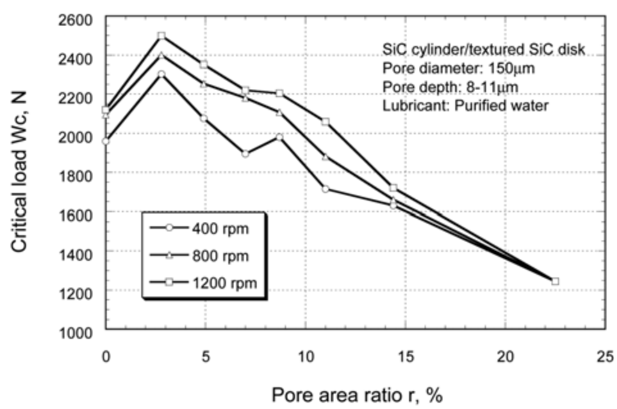

Fig. 12 The critical load after running-in with the loads that are as high as possible

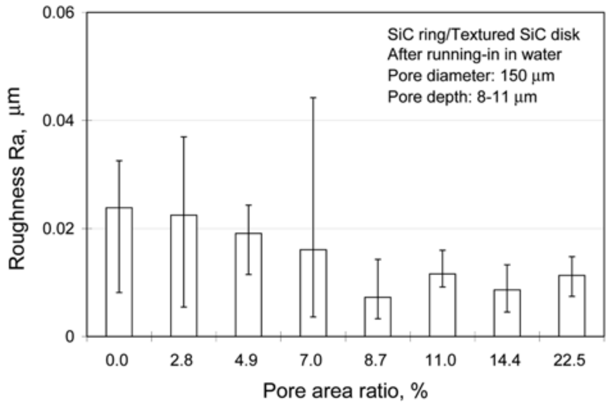

Fig. 13 The roughness of the surface around micro-pores after the running-in process

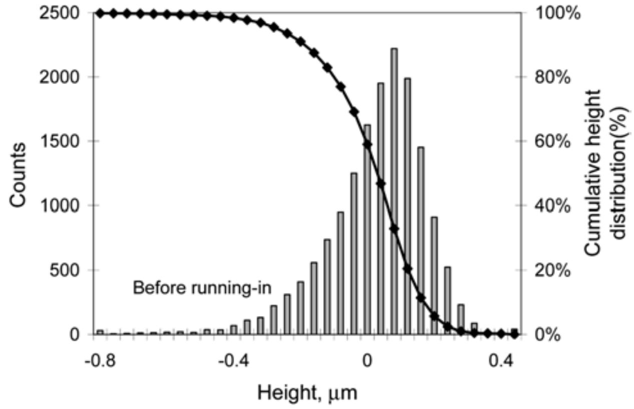

Fig. 14 The height distribution of the surface of SiC before running in

the surface. The deviation bar shows the roughness distribution on the whole surface.

It is found that different pore area ratios result in different surface roughnesses. Generally, the specimens with high pore area ratios have smooth surfaces after running in.

4 DISCUSSION

In reference [**13**], the effect of micropores on the critical load is analysed and discussed. The hydrodynamic pressure generated by micropores is supposed to be the main reason for increasing the critical load when the pore area ratio is lower than 10 per cent, and the rapid decrease in contact area due to the increase in pore area ratio accompanied by the increase in heat-affected area is considered to be the reason for the decrease in the critical load when the pore area ratio is higher than 10 per cent.

Therefore, this section will concentrate on a discussion about the effect of micropores during the running-in process.

Figure 14 shows the height distribution and the bearing curve of the SiC surface before running in. Figure 15 shows the changes in the bearing curve after the multi-step loading running-in process with maximum loads of 400 N and 800 N. The areas A_1 and A_2 surrounded by those curves present the wear volumes during the running-in processes of 0–400 N and 400–800 N respectively. Obviously, the wear volume represented by A_1 is much larger than that represented by A_2 although their load increments are the same up to 400 N. This agrees with the experiment results shown in Fig. 7 that the running-in speed is high in the initial stage and becomes increasingly slower with increase in the load. So at the end, even with increases in load and sliding time, the wear rate will become so slow that the improvement to the contact will not be obvious. This is the time to stop the running-in process in this experiment.

Comparing Figs 11 and 12, it can be said that a proper surface texture is more effective in improving the running-in ability of SiC than is an increase in the load-carrying capacity by hydrodynamic pressure.

For SiC contacts, water is not only a lubricant but also a necessary material for tribochemical reaction when they are sliding in water. A higher pore area ratio will give a better water supply which should help the progress of tribochemical wear. So a higher pore area ratio results in a smoother surface, as shown in Fig. 13. In other words, the running-in process is able to be carried out to a greater extent with a suitable surface texture.

It is shown that two parallel flat surfaces with a relative longitudinal motion do generate a pressure within the film. The load support W of this contact in the mixed-lubrication region is thus made up of

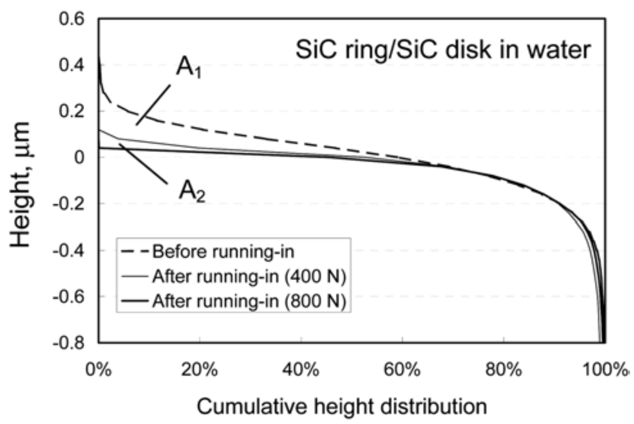

Fig. 15 The changes in height distribution of the SiC surface after the multi-step running-in process with maximum loads of 400 N (2.0 MPa) and 800 N (4.1 MPa)

a contact portion W_m and a fluid pressure portion W_f for the untextured specimens, according to

$$W = W_m + W_f \tag{1}$$

With a textured specimen there is additionally a hydrodynamic pressure portion W_t generated by surface texture, according to

$$W = W_m + W_f + W_t \tag{2}$$

Using a simple plastic contact model [**15**],

$$W_m = AP_c p_s \tag{3}$$

This indicates that a smooth surface has a high load-carrying capacity since it has a high probability of contact. This is an explanation for the result obtained by Wong *et al.* [**8**], namely that a smoother surface of SiC has a lower friction coefficient.

The mechanism of W_f is still unclear. By supposing that this mechanism has a functional form similar to that of a simple one-dimensional tilted pad slider bearing, the expression can be given as [**15**],

$$W_f = \frac{\eta U}{h_{min}^2} BL^2 f(L, B) \tag{4}$$

where the function $f(L, B)$ is meant to represent a wide range of functional possibilities but is in fact a function of film thickness ratio only in the one-dimensional slider.

The smoother surface generated by a higher running-in load is able to have a smaller h_{min} to increase the hydrodynamic portion W_f. As a result, the total load-carrying capacity W is increased, as shown in Fig. 9.

In Fig. 11, the specimens with pore area ratios below 12 per cent have almost the same running-in processes, which was carried out at 1000 r/min with a maximum load of 2000 N. The critical load does not vary very much at rotational speeds of 800 and 1200 r/min but decreases substantially with increase in pore area ratio at 400 r/min. This could be explained as arising because, after same running-in processes, they have almost same load-carrying capacities, irrespective of their pore area ratios. However, their portions of W_m and W_f are different since the portion W_t should vary according to the different pore area ratios. As a hydrodynamic pressure, W_t is related to the relative sliding speed. Therefore, when the rotational speed decreases to 400 r/min which is far from the running-in speed of 1000 r/min, W_t varies, resulting in the different critical loads.

Both equation (3) and equation (4) are related to the area for contact. So a high pore area ratio results in a decrease in the load-carrying capacity in the portions of W_m and W_f due to the decrease in contact area.

For the high pore area ratios of 14.4 per cent and 22.5 per cent, the surface becomes smooth, and a hydrodynamic pressure is generated; the contact area is decreased so much by pores that it does not generate any improvement in critical load compared with that of untextured specimens.

For the specimens with pore area ratios of 3–5 per cent, the contact area is not decreased very much due to the low pore area ratio. Because of the additional hydrodynamic pressure generated by the pores, and the smoother surface generated during the running-in process with the aid of the pores, as a result an improvement in the critical load is obtained.

5 CONCLUSIONS

The running-in process of water-lubricated SiC in a thrust-bearing-type contact was studied experimentally.

The running-in process obviously influences the load-carrying capacity of SiC sliding in water. To avoid brittle fracture and to keep the tribochemical wear as the dominant wear mode is the key point of the running-in process of SiC for the purpose of obtaining low friction.

The load-carrying capacity, which is measured as the critical load in this research, is directly related to the maximum running-in load. A higher running-in load, which can be realized by multi-step loading running-in process, is effective in generating a higher load-carrying capacity.

Micropores textured on the surface of SiC help to generate a smooth surface with tribochemical wear during the running-in process in water. This is one of the mechanisms of increasing the load-carrying capacity of SiC in water by surface texture.

REFERENCES

1 **Nau, B. S.** Mechancal seal face materials. *Proc. Instn Mech. Engrs, Part J: J. Engineering Tribology*, 1987, **211**, 165–183.
2 **Asanabe, S.** Applications of ceramics for tribological components. *Tribology Int.*, 1987, **20**(6), 355–364.
3 **Andersson, P.** and **Lintula, P.** Load-carrying capability of water-lubricated ceramic journal bearings. *Tribology Int.*, 1994, **27**(5), 315–321.
4 **Tomizawa, H.** and **Fischer, T. E.** Friction and wear of silicon nitride and silicon carbide in water: hydrodynamic lubrication at low sliding speed obtained by tribochemical wear. *ASLE Trans.*, 1987, **30**(1), 41–46.

5 **Sasaki, S.** The effects of water on friction and wear of ceramics. *J. Japan Soc. Lubric. Engrs*, 1988, **33**(8), 620–628.

6 **Andersson, P., Juhanko, J., Nikkila, A. P.,** and **Lintula, P.** Influence of topography on the running-in of water-lubricated silicon carbide journal bearings. *Wear*, 1996, **201**(1–2), 1–9.

7 **Andersson, P., Nikkila, A. P.,** and **Lintula, P.** Wear characteristics of water-Lubricated SiC journal bearings in intermittent motion. *Wear*, 1994, **179**(1–2), 57–62.

8 **Wong, H. C., Umehara, N.,** and **Kato, K.** The effect of surface roughness on friction of ceramics sliding in water. *Wear*, 1998, **218**(2), 237–243.

9 **Hsu, S. M.** and **Shen, M. C.** Ceramic wear maps. *Wear*, 1996, **200**, 154–175.

10 **Xu, J., Kato, K.,** and **Hirayama, T.** The transition of wear mode during the running-in process of silicon nitride sliding in water. *Wear*, 1997, **205**, 55–63.

11 **Chen, M., Kato, K.,** and **Adachi, K.** The comparisons of sliding speed and normal load effect on friction coefficients of self-mated Si_3N_4 and SiC under water lubrication. *Tribology Int.*, 2002, **35**, 129–135.

12 **Chen, M., Kato, K.,** and **Adachi, K.** Friction and wear of self-mated SiC and Si_3N_4 sliding in water. *Wear*, 2001, **250**, 246–255.

13 **Wang, X., Kato, K., Adachi, K.,** and **Aizawa, K.** The effect of laser texturing of SiC surface on the critical load for the transition of water lubrication mode from hydrodynamic to mixed. *Tribology Int.*, 2001, **34**, 703–711.

14 **Wang, X., Kato, K.,** and **Adachi, K.** The lubrication effect of micro-pits on parallel sliding faces of SiC in water. *Tribology Trans.*, 2002, **45**(3), 294–301.

15 **Lebeck, A. O.** Parallel sliding load support in the mixed friction regime. 1: the experimental data. *Trans. ASME, J. Tribology*, 1987, **109**(1), 189–195.

APPENDIX

Notation

A	area of contact (m^2)
B	bearing width (m)
h_{min}	minimum film thickness (m)
L	bearing length (m)
P_c	probability of contact (per cent)
p_s	flow pressure (hardness) of the weaker material (Pa)
r	pore area ratio (per cent)
R_a	average roughness (μm)
U	sliding speed (m/s)
W_c	critical load for the transition from hydrodynamic to mixed lubrication (N)
W	load support (N)
W_m	contact portion of the load support (N)
W_f	fluid pressure portion of the load support (N)
W_t	hydrodynamic pressure portion of the load support generated by the surface texture (N)
μ	friction coefficient
η	viscosity of lubricant (Pa s)